PROCEEDINGS, Thirty-Sixth Workshop on Geothermal Reservoir Engineering
Stanford University, Stanford, California, January 31 - February 2, 2011
SGP-TR-191

ASSESSING THE GEOCHEMICAL IMPACT OF INJECTION OF COOLED TRIASSIC BRINES INTO THE DOGGER AQUIFER (PARIS BASIN, FRANCE): A 2D REACTIVE TRANSPORT MODELING STUDY

C. Castillo, C. Kervévan, N. Jacquemet, V. Hamm, V. Bouchot, B. Sanjuan

B.R.G.M
3, avenue Claude Guillemin - BP 36009
Orléans cedex 02, 45060, France
e-mail: c.castillo@brgm.fr

ABSTRACT

The Triassic sandstone reservoirs of the Paris Basin (France) have attractive geothermal potential for district heating. However, previous exploitations of these reservoirs have revealed re-injection problems preventing from further geothermal operations. To avoid these crucial problems, a possible option would be to inject the exploited Triassic brines in the Dogger aquifer characterized by better re-injection properties. However, this solution might trigger geochemical reactions that may impact negatively the properties of the Dogger aquifer, notably its porosity.
This study, based on numerical simulations, aims to identify and quantify the possible consequences of the thermo-hydro-geochemical processes induced by the re-injection of the cooled Triassic brines into the Dogger aquifer.
Initial batch simulations show potential occurrences of precipitation/dissolution reactions that could potentially impact the Dogger porosity: dissolution of disordered dolomite and calcium sulfate; precipitation of silicates, barium sulfate and sulfides.
In a second step, 2D reactive transport modeling was performed. The results obtained up to now suggest that the impact of the Triassic re-injection could be limited to the first fifty meters around the injection well and be insignificant in terms of porosity variation (< 0.14 percentage point). However, at this stage, species which are sensitive to redox conditions, such as iron and sulfur, are not yet considered. Therefore, this reactive transport model does not take into account some of the reactions identified in the batch modeling as potentially induced during the Triassic re-injection into the Dogger, such as barium sulfate and sulfides precipitation. This is planned to be done in upcoming modeling tasks.

INTRODUCTION

Geothermal exploitation in the Paris basin (France) started in the 1970s. Since, the carbonate Dogger aquifer (1.500-2.000 m deep) remains the main target. But, to satisfy the current energetic demand, finding new geothermal resources is a crucial issue. The previous study (CLASTIQ-1 project, Bouchot *et al.*, 2008) has shown that the Triassic sandstone reservoirs of the Paris basin (2000 to 3000 m deep) have attractive geothermal potential for district heating as an alternative to the Dogger aquifer. However, previous exploitations of these sandstone reservoirs have revealed re-injection problems preventing from further geothermal operations. To overcome these technical difficulties, one possible solution envisaged would be to inject (totally or partly) the exploited Triassic brines in another aquifer with better re-injection properties, namely the Dogger aquifer. However, this solution might trigger geochemical reactions that risk damaging the properties of the Dogger, in particular its porosity. The objective of the modeling work presented here is to identify physical and chemical processes induced by the re-injection of the cooled Triassic brines into the Dogger aquifer, and quantify their possible consequences on the Dogger porosity. This study was conducted in the framework of the CLASTIQ-2 project, co-funded by the French Environment and Energy Management Agency (ADEME) and BRGM.

DATA AVAILABLE

Formations water

The chemical compositions of both the Triassic and the Dogger formations waters are relatively well known at present, owing to their exploitation for oil, gas and geothermal energy.

In 2008, field investigations were carried out by Lopez and Millot (2008) within the Paris basin. Several samples were taken from the Triassic formations waters and detailed chemical (major and trace elements) and isotopic (^{18}O, ^{2}H, *etc.*) analysis were performed. The chemical compositions of two of the samples collected for the Lopez and Millot (2008) study are selected here as representatives for the Triassic formations of the Paris basin. The injection of the cooled Triassic brines into the Dogger aquifer will be performed near the Triassic production well. Consequently, the chemical data used for the Dogger formation water come from two geothermal production wells, CGO1 (Rojaz *et al.*, 1989) and Melun 83 (Michard and Bastide, 1988), located in the vicinity of the Triassic sampling points considered (Figure 1, Table 1). Besides, the chemical data are considered by couple Triassic/Dogger in this study (Table 1).

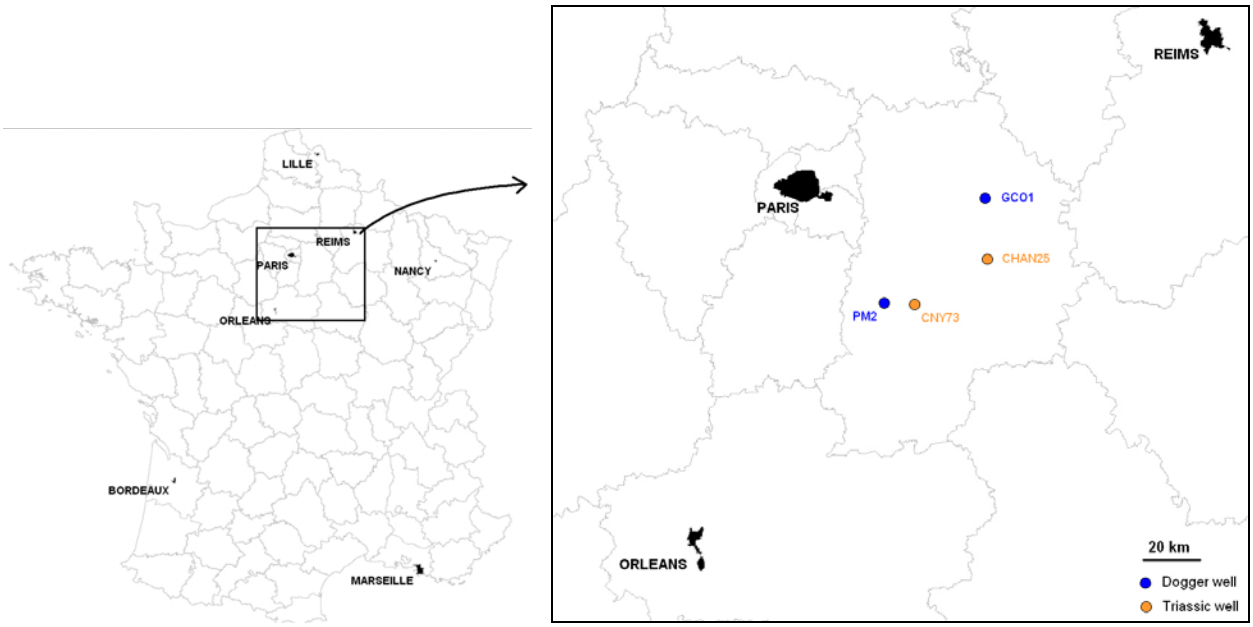

Figure 1 : Location map of the chemical data used in this study.

Table 1 : Chemical data sets considered.

Data couple	Well ID	Location	X*(m)	Y*(m)	Depth(m)	Aquifer
1	CHAN25	Champotran	656588	2406776	2473	Triassic
	CGO1	Coulommiers	655951	2425247	1710	Dogger
2	CNY73	Chaunoy	634507	2393235	2239	Triassic
	PM2	Melun	625423	2393582	1940	Dogger

*Lambert II extended coordinates

The chemical compositions of the fluids used in this study are given in Table 2 and in Table 3 for the Triassic and the Dogger formations respectively. Contrary to those of the Trias, the Dogger brines examined in this study show a significant variability of their composition: the Dogger brines studied have TDS (total dissolved salts) values ranging from 13 g/l to 35 g/l whereas the two Triassic brines both have comparable TDS values around 120 g/l.

Table 2 : Chemical compositions of the Triassic formation brines (Lopez et al., 2008).

	Chaunoy CNY73	**Champotran** CHAN25	
pH	6	6.5	
Na	36700	36200	mg/l
K	972	952	mg/l
Mg	1068	1010	mg/l
Ca	5841	5600	mg/l
Cl	73500	72000	mg/l
SO4	704	685	mg/l
Cinorg. (HCO3)	7.5	7.3	mg/l
TDS	120	118	g/l
Br	673	633	mg/l
NH4	62	63.3	mg/l
F	< quantification limit	0.7	mg/l
SiO2	49.6	40.3	mg/l
Al	22.2	64.7	µg/l
B	52	58	mg/l
Ba	2278	2299	µg/l
Fe	18.7	5.72	mg/l
Li	40	36.3	mg/l
Mn	1396	1295	µg/l
Pb	80	11	µg/l
Sr	300	287	mg/l
Zn	482	302	µg/l

Table 3 : Chemical compositions of the Dogger formation water (Rojaz et al., *1989 ; Michard and Bastide, 1988).*

	Melun PM2	**Coulommiers** GCO1	
pH	6.2	6.24	
Na	3969	10181	mg/l
K	69.48	142	mg/l
Mg	148	356	mg/l
Ca	578	1763	mg/l
Cl	7200	19489	mg/l
SO4	956	1310	mg/l
HS	9.40	1.63	mg/l
Alkalinity	309.79	266	mg/l
TDS	13	33	g/l
Br	41.38	78.16	mg/l
N	16.15	27.99	mg/l
F	4.24	0.63	mg/l
SiO2	40.88	45.36	mg/l
Al	7.12	6.13	µg/l
B	9.00	17.98	mg/l
Ba	157.6	51.09	µg/l
Fe	0.11	6.10	mg/l
Li	1.48	2.64	mg/l
Mn	Not analyzed	61.30	µg/l
Sr	32.92	59.61	mg/l

Mineralogy of the Dogger formation

The representative mineralogy of the Dogger aquifer considered in this work is based on data available in the literature (Rojaz *et al.*, 1989). It is mainly composed of carbonates (80% in mass fraction) with silicates and sulfate. The sulfate content varies with the location (Table 4).

Table 4 : Dogger aquifer mineralogy.

Mineral	**Mass percent**	
	Melun region	Coulommiers region
Calcite	70	70
Disordered dolomite	10	10
Quartz	5	5
Albite	5	5
K-Feldspar	5	5
Barite	5	0
Anhydrite	0	5

METHODOLOGY AND NUMERICAL TOOLS

A summary of the modeling work undertaken in this study is presented in

Table 7, where the objectives of each step described below are particularly highlighted.

Methodology

The injection of the cooled Triassic brines into the Dogger aquifer will cause the mixing between two brines with contrasted compositions and temperatures

(the Triassic brines is planned to be injected at 40°C). Thus, it will disturb the initial thermodynamic equilibrium between the Dogger aquifer phases (water and rock), and will lead geochemical reactions which can affect the reservoir porosity. To access this possibility, this modeling work is divided into four main stages of increasing complexity:

1) Construction of consistent chemical compositions for the cooled Triassic fluids planned to be injected,
2) Mixing batch modeling without any precipitation/dissolution processes being considered,
3) Mixing batch modeling integrating mineral dissolution and precipitation kinetics,
4) 2D reactive transport modeling.

The specific objective of each of these steps is summarized in

Table 7 and detailed in the following paragraphs.

Calculation of the cooled Triassic brine composition

The chemical compositions of the Triassic formation brines presented previously are taken as starting points. Then a series of batch calculations (one for each sampling location, *i.e*. Chaunoy and Champotran) are carried out to prescribe thermodynamic equilibrium with calcite and kaolinite (two usual minerals of the Triassic formations) at 100°C (temperature representative for the area of interest of the Triassic reservoir). Subsequently, water cooling down to 40°C is simulated. Equilibration of water with a selection of minerals present in the reservoir is commonly used to access a chemical composition of the formation water more consistent with the reservoir mineralogy. The chemical compositions of the Dogger formation waters were already consistent with the Dogger mineralogy. Thus, this equilibration step was not necessary.

Mixing batch modeling

Batch modeling is used to identify the mineral reactions that can occur due to the Triassic brines injection into the Dogger aquifer, without taking into account any hydrodynamic process and water flux. As a simplified approach to approximate the spatial variability of the water composition from the immediate vicinity of the injection well to the far field, several mixing rates between the Triassic and the Dogger end-members were simulated.

The first step of these batch simulations aims at identifying the thermodynamic state of the mixed waters investigated; for that purpose, only saturation indexes of mineral phases of interest are observed as indicators of their potential reactivity. In a second step, primary and potential secondary mineral dissolution and precipitation processes are taken into account in a kinetic approach in order to consider the reaction paths likely triggered by the mixing effect (for details see appendix).

Reactive transport modeling

Reactive transport modeling adds the spatial dimension to the results previously obtained. Now taking into account both the actual water fluxes as well as the spatial distribution makes it possible to localize and quantify the impact of the water/rock reactivity in terms of porosity variation within the Dogger reservoir.

As a first approach, we did not consider any spatial heterogeneity within the Dogger aquifer. Consequently, a 2D radial geometry centered around the injection well was considered to be adapted to model this problem.

As illustrated in Figure 2, the reservoir is approximated by a horizontal porous layer with homogeneous physical and chemical properties. In order to take into account more accurately the heat exchange processes, the reservoir was assumed to be surrounded by both an upper and a lower horizontal impermeable layers of known thermal properties. The model thus accounts for thermal, hydraulic and chemical processes involved in this injection problem. The hydraulic and the thermal parameters used for these simulations are indicated in Table 5. All chemical parameters are identical to those used for the kinetic batch modeling.

Table 5: Hydraulic and thermal parameters used for the reactive transport modeling.

	Productive layer	**Surrounding layers**
Thickness (m)	10	200
Intrinsic permeability (D)	3.5	1.10^{-6}
Porosity (%)	15	1
Volumetric heat capacity ($MJ/m^3/K$)	2.5	2.2
Heat conductivity	2.5	2

(W/m/K)		
Longitudinal dispersivity (m)	20	20
Transversal dispersivity (m)	10	10

The maximal radial extent is 5 km. The mesh is composed of 1792 cells. It is refined vertically around the injection well and horizontally near the boundaries between the reservoir and the impermeable layers to minimize numerical errors calculating the geochemical processes occurring in the well field and heat exchanges. The grid spacing varies from 1.25 m in the first 10 m around the well to 10 m in the 10-600 m zone, and finally to 100 m in the 600-5,000 m.

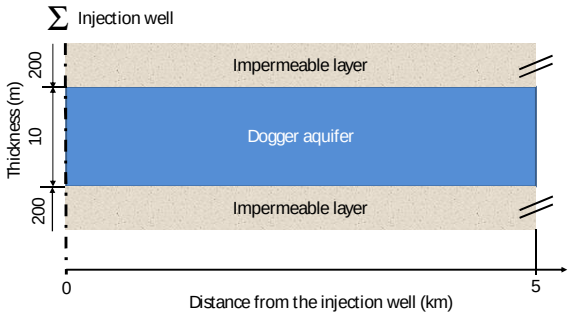

Figure 2 – 2D radial geometry used for reactive transport modeling

Two injection options were considered in the simulations (Table 6):

- injection of all the Triassic brines exploited(150 m^3/h),
- injection of only a part of the Triassic brines exploited (75 m^3/h).

Simulations were performed over an 8 months period (*i.e.* during one heating period).

Table 6 : Injection scenarios examined during the reactive transport modeling.

	1st scenario	**2nd scenario**
Flow rate (m^3/h)	150	75
Temperature of injection of the Triassic brines (°C)	40	40
Duration of the injection period (month)	8	8

Numerical tools

The Triassic brines are highly saline (TDS around 120 g/l). Thus, the Pitzer approach is clearly the optimal choice for this problem (as the mixture TDS likely to be encountered will be greater than that of seawater - typically 35 g/l -). Figure 3 illustrates, for NaCl, that the impact of salinity (expressed in ionic strength on this graph) on the activity coefficient value is significant beyond seawater concentrations, compared to other activity models only applicable to low salinity values.

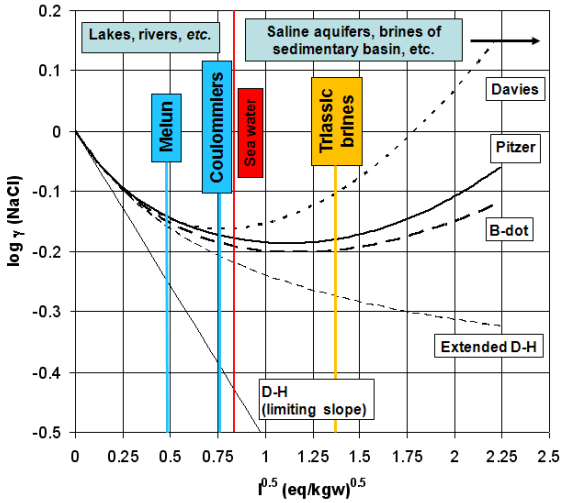

Figure 3 : Variations of the logarithm of the mean activity coefficient of NaCl as a function of the square root of the ionic strength, according to different activity coefficient models (Davies, Pitzer, B-dot and extended Debye-Hückel).

However, the thermodynamic databases based on the Pitzer model described in the literature are generally limited in species taken into account and in temperature range. As a result, none of the currently available databases is totally appropriate for the problem examined. Consequently, to evaluate the uncertainties associated with the choice of the activity coefficient model, we performed all the batch simulations (including those for the calculation of the cooled Triassic brine) with three different databases:

- two of them are based on the B-dot model (Helgeson *et al.*, 1981): Thermoddem (Blanc *et al.*, 2009), and llnl.dat (Parkurst and Appelo, 1999),
- the third one is based on the Pitzer approach. It has been developed at BRGM for problems involving very high saline brines (up to 300 g/l) at high (P,T) conditions, but is still not validated for aluminum speciation at neutral pH and high temperature (Azaroual *et al.*, 2004).

The reactive transport simulations are performed using only one database, EQ36.dat (an llnl.dat equivalent), because there is currently no Pitzer database available for the numerical code used for this modelling (MARTHE-REACT; Thiéry *et al.*, 2009). MARTHE-REACT is an extension of MARTHE (Thiéry, 1991), which has been upgraded by coupling with the geochemical module of TOUGHREACT (Xu *et al.*, 2004).

Therefore, the batch simulations (including the construction of the Triassic cooled down) were carried out using the following geochemical codes:

- PHREEQC associated with the databases Thermoddem and LLNL.dat and,
- SCALE2000 (Azaroual *et al.*, 2004) with its own Pitzer included database.

On the other hand, the coupled modeling was performed using the Thermo-Hydraulic-Chemical coupled code MARTHE-REACT and the EQ36.dat database.

Table 7 : Summary of the main modeling tasks undertaken in this study.

Objectives	Stage	Modeling method	Numerical code	Database	Observed parameters
Calculate the chemical composition of the cooled Triassic end-member	**1**	Batch	PHREEQC	Thermoddem and LLNL.dat	
			SCALE2000	SCALE2000 attached Pitzer database	
Identify the main geochemical reactions, such as the possible precipitation of secondary phases	**2**	Batch	*id.* to stage 1	*id*. to stage 1	Minerals saturation index (SI)
Have an idea of the potential reactions path, and more generally, increase the accuracy of the first predictions (stage 2) on the geochemical reactivity of the "mixed waters" and the-Dogger minerals.	**3**	Batch + Mineral precipitation and dissolution kinetics (including identified possible secondary phases)	*id*. to stage 1	*id*. to stage 1	Amounts of precipitated or dissolved minerals + sulfides (mackinawite, pyrite, galena *etc.*) SI
• Assess the impact of the cooled Triassic brines injection on the reservoir porosity • Better understand the behavior of the injection well field	**4**	2D reactive transport	MARTHE-REACT	EQ36.dat	Volume of precipitated or dissolved minerals + reservoir porosity

RESULTS AND DISCUSSION

The Triassic end-members

The compositions of the Triassic brines for the two sites considered (Chaunoy and Champotran) are very similar. On the contrary, the compositions of the Dogger waters vary significantly with the site considered. As an illustration of the differences induced by the activity model selected, we present in Table 8 the chemical composition of the cooled Triassic brine calculated for the Chaunoy/Melun dataset, using all the numerical tools and associated databases described previously. The results presented in Table 8 show significant differences, mainly for chemical elements (Ca, C, Si, Al) directly involved in the thermodynamic equilibriums (calcite, kaolinite) prescribed in our initial calculations, before simulating the cooling of the brine itself. Moreover, in SCALE2000, the density of the solution is accurately calculated as a function of the actual speciation of the brine; consequently, conversions from initial mg/l data to mol/kgw are responsible for some small discrepancies in molality values. The strongest discrepancies are observed for aluminum concentration; this is mainly explained by still uncompleted Pitzer data in the context of neutral pH solutions. However, except for aluminum, the compositions calculated here are globally consistent one with another.

Table 8 : Chemical composition of the cooled Chaunoy Triassic brine calculated with PHREEQC (Thermoddem.dat and llnl.dat), and SCALE2000 (Pitzer database) at 40°C. All units are in mol/kgw except for TDS (g/l) and density (g/cm^3).

	PHREEQC Thermoddem	**PHREEQC llnl.dat**	**SCALE2000 Pitzer**
pH	6.70	6.64	6.53
Na	1.658e+000	1.658e+000	1.662E+000
K	2.582e-002	2.582e-002	2.588E-002
Mg	4.563e-002	1068	4.574E-002
Ca	1.524e-001	1.524e-001	1.517E-001
Cl	2.154e+000	2.154e+000	2.158E+000
SO4	6.798e-003	7.614e-003	7.628E-003
$C_{inorg.}$	1.117e-003	1.112e-003	2.648E-004
Br	8.749e-003	8.749e-003	8.767E-003
NH_4	3.570e-003	3.570e-003	3.577E-003
F	0	0 limit	0
SiO_2	8.568e-004	8.571e-004	8.584E-004
Al	1.386e-007	2.790e-007	2.847E-008
B	4.996e-003	4.996e-003	N/A
Ba	1.723e-005	1.723e-0052278	1.727E-005
Fe	3.478e-004	3.478e-004	3.485E-004
Li	5.988e-003	5.986e-003	5.998E-003
Mn	2.640e-005	2.640e-005	N/A
Pb	4.011e-007	4.011e-007	N/A
Sr	3.557e-003	3.557e-003	3.564E-003
Zn	7.659e-006	7.657e-006	N/A
TDS	120	120	119.3
Density	N/A	N/A	1.075

Mixing batch modeling results

The results of the first batch modeling (stage 2) are partly illustrated on Figure 4 (for sake of clarity, only calcite, barite, and kaolinite are represented). They show that the injection of cooled Triassic brines into the Dogger aquifer could potentially induce mineral precipitation and dissolution reactions that, at the end, could impact the reservoir porosity:

- dissolution (IS < 0.3) of some Dogger minerals such as carbonates (calcite and dolomite) and calcium sulfate,
- precipitation (IS > 0.3) of silicates, barium sulfate (barite) and sulfides.

These general trends are globally similar whatever the Trias/Dogger data set considered. The same remark can be made for the numerical tools (code/database) employed, except for minerals containing aluminum (such as kaolinite) where, unsurprisingly, significant discrepancies are observed. However, the proportion of mixing for which the tendencies emerge depends on both the data set and the tools used. Thus, barium sulfate can precipitate if the mixing rate is less than 80% of Dogger water according to the simulations performed with PHREEQC/llnl.dat, whereas it can precipitate at higher mixing percentage (95% of Dogger fluid) according to PHREEQC/Thermoddem and SCALE2000. This example illustrates the importance of the choice of the activity model used in the calculation.

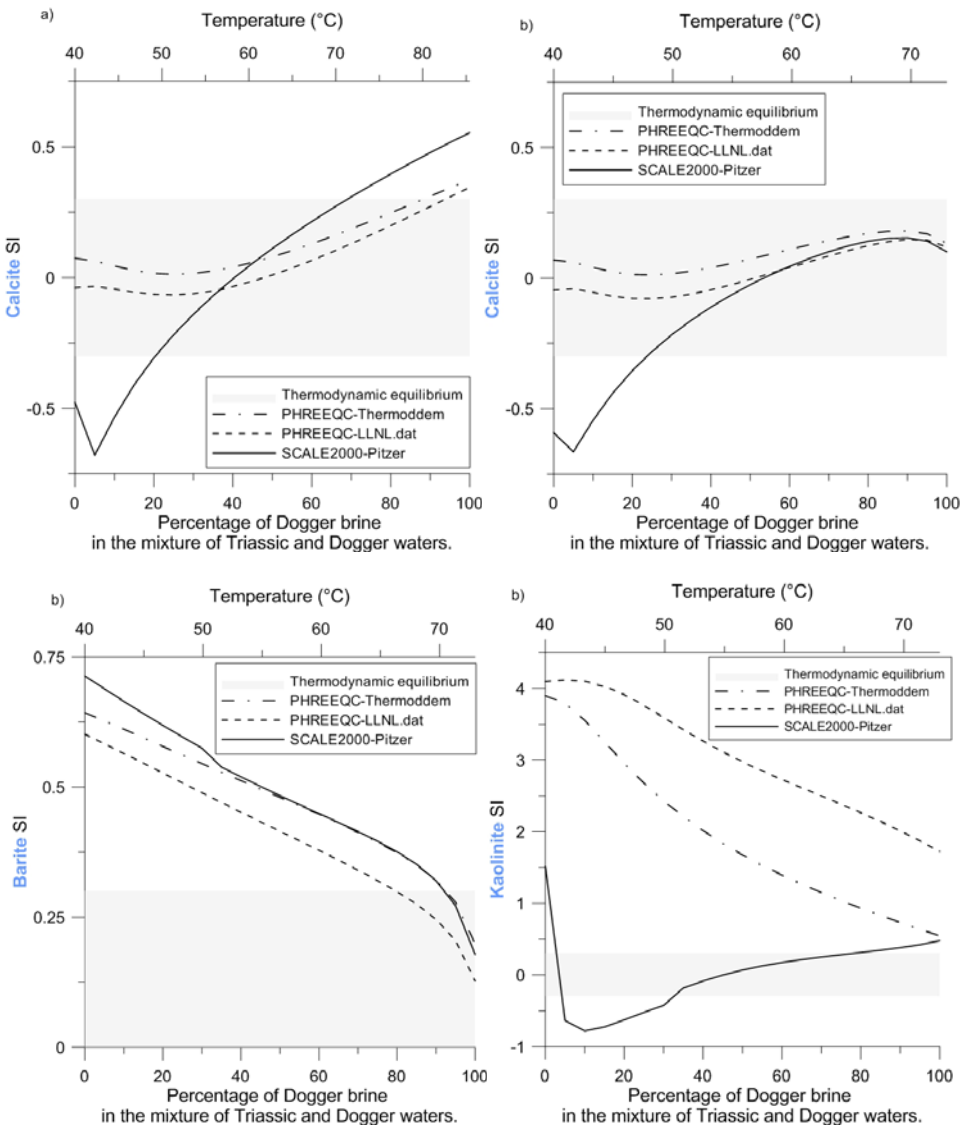

Figure 4 : Mixing batch modeling (2nd stage) – Evolution of the saturation index (SI) of a few minerals (calcite, barite and kaolinite) during the mixing of Dogger and Triassic brines – Results obtain with the data couple a) Champotran/Coulommiers and b) Chaunoy/Melun.

The second batch modeling (stage 3) now takes into account the mineral precipitation and dissolution kinetics (including those of the potential secondary mineral phases, for details see appendix 1). The results are summarized in Table 9. They confirm overall the results of the first modeling stage. Actually, only the reactivity of calcite and albite differ: albite could dissolve due to the Triassic injection whereas calcite could be stable. Additionally, these results inform on the potential reactions path. Thus, it appears that the stability of calcite is related to the Dogger dolomite alteration which notably releases Ca^{2+} and HCO_3^- ions.

Table 9 : Mixing batch modeling (3rd stage) – Mineral reactions induced by the injection of cooled Triassic brines into the Dogger aquifer.

	Calculated reactivity for various Triassic/Dogger mixing rates (expressed in % of Dogger water)					
Minerals	**0**	**20**	**40**	**60**	**80**	**100**
Calcite	0	0	0	0	0	0
Disordered dolomite	–	–	–	– **0**	0	0
Quartz	0	0	0	0	0	0
Albite	–	–	–	0	0	0
K-Feldspar	+	+	+	+	+	0
Barite	+	+	+	+ **0**	0	0
Anhydrite	**0** **–**	**0** **–**	**0** **–**	0	0	0
Magnesite	0	0	0	0	0	0
Chalcedony	+	+ **0**	0	0	0	0
Gibbsite	+	+	+	+	+ **0**	0
Clays *(Kaolinite, Illite et Montmorillonite-Na)*	+	+	+	+	+	0
Sulfides *(Mackinawite)*	+	+	+	+	+	+

Legend

+: precipitation

-: dissolution

0: none

Results in black: identical for each data couples (Chaunoy/Melun and Champotran/Coulommiers).

Results in blue: specific to the Chaunoy/Melun data set

Results in red: specific to the Champotran/Coulommiers data set

Reactive transport modeling

This last stage of the study is still in progress. For the moment, the species sensitive to redox conditions (such as iron and sulfur) had to be removed of the system due to unexpected MARTHE-REACT convergence problems. More precisely, the simulations performed up to now only take into account the aqueous and mineral species which are not highlighted in grey in Table 3, Table 8, and

Table 9. The main results of the reactive transport modeling are illustrated in Figure 5 and summarized in Table 10. The geochemical processes induced by the injection of cooled Triassic brines into the Dogger are similar whatever the injection scenario performed (*i.e*. whatever the flow rate considered). However, the quantities involved differ: they are more important in the first scenario (*i.e.* when the Triassic brines exploited are assumed to be totally injected into the Dogger aquifer). Thus, for sake of clarity, Figure 5 only concerns the results obtained with the first scenario, and Table 10 presents the mineral quantities involved in each scenario.

The results show that the cooled Triassic brines injection may induce dissolution of the Dogger disordered dolomite in the first fifty meters around the injection well (up to 14 L per m^3 of porous medium). This dissolution is accompanied by calcite precipitation which can be significant, depending on the data set used (up to 14.6 L/m^3 according to the simulations performed with the Chaunoy/Melun data set). In this latter case, it appears that most of the disordered dolomite dissolved in the first meters around the well precipitates in calcite. The cooled Triassic brines injection may also cause some clay precipitation (Montmorillonite-Na notably) in the first fifty meters around the well, however, the quantities involved are negligible (< 0.5 m L per m^3 of porous medium). As a result, the impact of these reactions on the reservoir porosity is limited to the well field and is insignificant (variation < 0.14 percentage point). However, it depends on the data set used: the porosity slightly increases according to the simulations performed with the first data set whereas it slightly decreases according to those carried out with the second one. In fact, it appears that the impact depends on the initial saturation of the Dogger fluids in carbonates (calcite and disordered dolomite) which slightly differs with the location (see Table 11).

Table 10 : Values of the maximum variations induced by the Triassic injection depending on the data used and the scenario simulated.

	Data set #1		**Data set #2**		Units
Scenario	1	2	1	2	
Disordered. dolomite	-1.4	-1.1	-14	-12.5	L/m^3 of porous medium
Calcite	+0.0045	+0.003	+14.7	+13.1	L/m^3 of porous medium
Montmorillonite-Na	+0.075	+0.022	+0.47	+0.16	mL/m^3 of porous medium
Porosity	+0.14	+0.11	-0.08	-0.07	percentage point

Table 11 : Initial saturation of the Dogger fluids in carbonates (calcite and disordered dolomite) – calculated using MARTHE-REACT and EQ36.dat

	Coulommiers CGO1	**Melun** PM2
Calcite	0.35	0.06
Disordered dolomite	0.43	-0.13

Data set #1 (Champotran/Coulommiers)	**Data set #2** (Chaunoy/Melun)

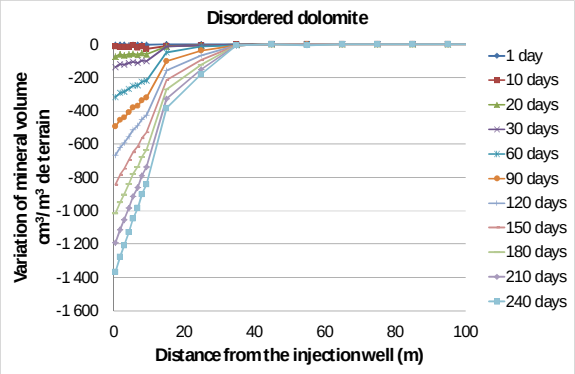

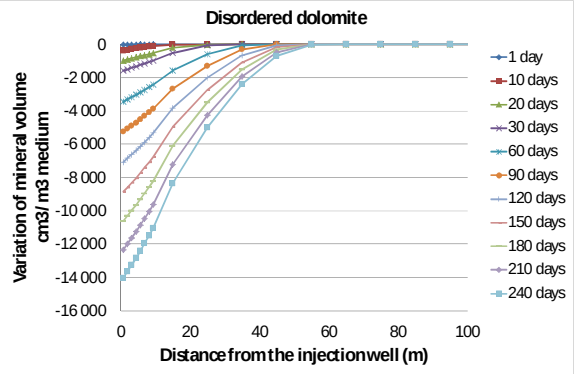

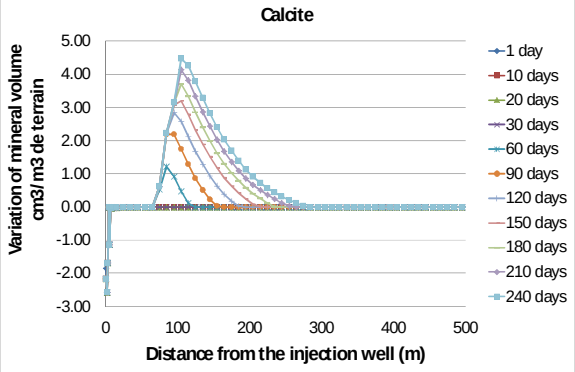

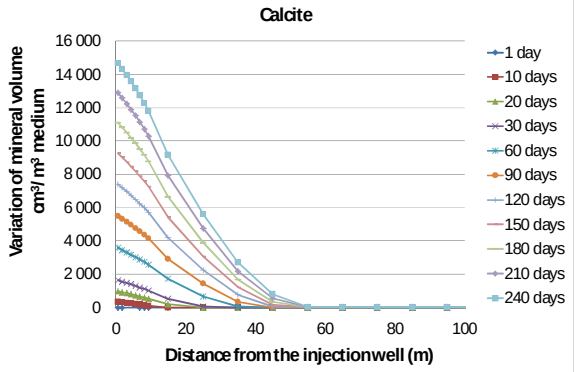

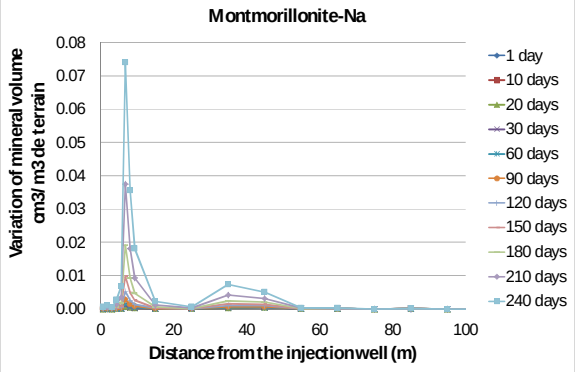

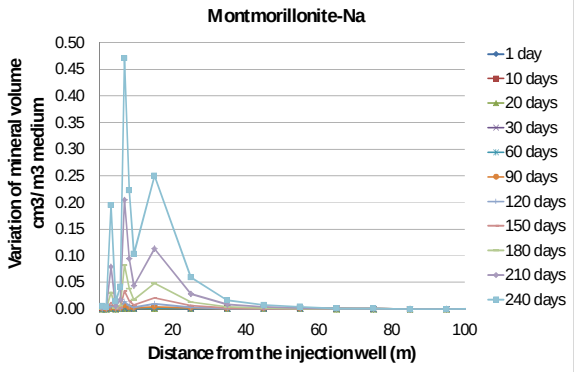

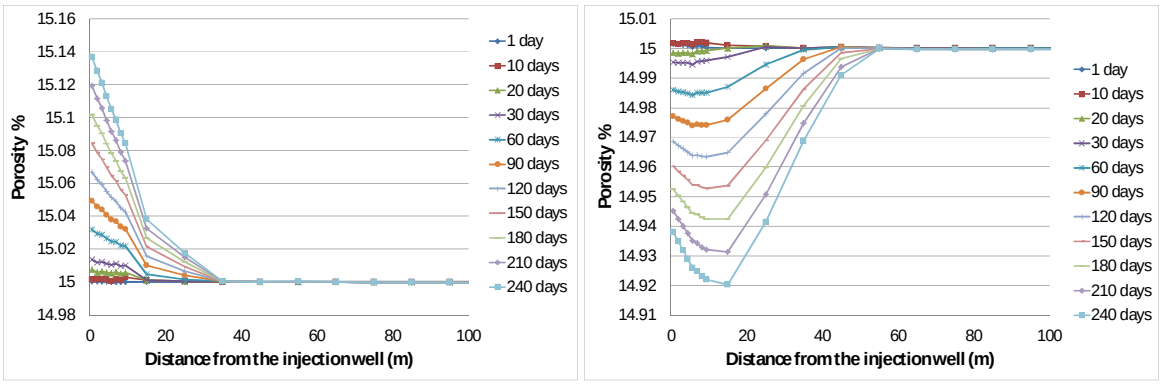

Figure 5 : Reactive transport modeling - Variation of mineral volume and of Dogger reservoir porosity induced by the cooled Triassic brines injection.

CONCLUSION

Batch modeling show that the injection of cooled Triassic brines into the Dogger aquifer may induce mineral precipitation and dissolution reactions:

- dissolution of some Dogger minerals such as disordered dolomite and calcium sulfate,
- precipitation of silicates (chalcedony and clays), barium sulfate and sulfides.

Reactive transport modeling performed up to now reveals that the impact of the Triassic re-injection could be limited to the first fifty meters around the injection well and be insignificant in terms of porosity variation (< 0.14 percentage point). In fact, it shows that the re-injection could mainly cause a slight dissolution of the Dogger disordered dolomite around the injection well and, in some case, a subsequent slight precipitation of calcite. However, it has to be mentioned that only one cycle of injection (over an assumed heating period of 8 months) was simulated; it would be interesting in future simulations to consider scenarios including several successive injection/release periods. Additionally, an important drawback of the performed simulations is that species which are sensitive to redox conditions, such as iron and sulfur, are not yet considered. Therefore, this reactive transport modeling does not take into account some of the reactions identified in the batch modeling as potentially induced during the Triassic re-injection into the Dogger, such as barium sulfate and sulfides precipitation. Upcoming modeling work will focus on the integration of redox sensitive species in the reactive transport model to provide a more reliable quantification of the reactive processes induced, and their impact on the reservoir porosity.

REFERENCES

Azaroual, M., Kervévan, C., Durance, M. V., Brochot, S. (2004), "SCALE2000 (v3.1), manuel utilisateur", BRGM ISBN 2-7159-0939-X.

Blanc, P., Lassin, A. and Piantone, P. (2009), http://thermoddem.brgm.fr/.

Bouchot, V., Bialkowski, A., Lopez, S., Ossi, A., Chiles, J., P., Garibaldi, C. and Jorand, C. (2008), "Evaluation du potentiel géothermique des réservoirs clastiques du Trias du Bassin de Paris", BRGM report RP-56463-FR.

Helgeson, H. C., Kirkham, D. H., Flowers, D. C. (1981), "Theoretical prediction of the thermodynamic behaviour of aqueous electrolytes at high pressures and temperatures: IV. Calculation of activity coefficients, osmotic coefficients, and apparent molal and standard and relative partial molal properties to 600°C and 5 kb", Am. J. Sci., 281, 1249-1516.

Kohler, S., Dufaud, F., Oelkers, E. H. (2003), "An experimental study of illite dissolution kinetics as a function of pH from 1.4 to 12.4 and temperature from 5 to 50°C", Geochimica and Cosmochimica Acta, 67, 3583-3594.

Lasaga, A. C. (1984), "Chemical kinetics of water-rock interaction", J. Geophys. Res., 89, 4009-4025.

Lopez, S. and Millot, R. (2008), "Problématique de reinjection des fluides géothermiques dans un reservoir argilo-gréseux : retour d'expériences et apport de l'étude des fluides du Trias du Bassin de Paris", BRGM report RP-56630-FR, 197p.

Michard, G. and Bastide, J. P. (1988), "Étude géochimique de la nappe du Dogger du Bassin parisien", Journal of volcanology and Geothermal Research, 35, 151-163.

Palandri, J. L. and Kharaka, Y. K. (2004), "A compilation of rate parameters of water-mineral interaction kinetics for application to geochemical modelling", U.S. Geological Survey Report 2004-1068.

Parkurst, D. L. and Appelo, C. A. J. (1999), "User's guide to PHREEQC (version 2). A computer program for speciation, batch-reaction, one-dimensional transport, and inverse geochemical calculations", Water-Resources Investigations Report 99-4259, 312p.

Rojaz, J., Giot, D., Le Nindre, Y. M. et al. (1989), "Caractérisation et modélisation du réservoir géothermique du Dogger (Bassin parisien, France)", BRGM report RR-30169-FR.

Thiéry, D. (1991), "Software MARTHE: 3 dimensional groundwater model", BRGM report R-32548, 201 p.

Thiéry, D., Jacquemet, N., Picot-Colbeaux, G., Kervévan, C., André, L., Azaroual, M. (2009), "Validation of MARTHE-REACT coupled surface and groundwater reactive transport code for modeling hydrosystems", in TOUGH symposium 2009 - 14-16/09/09 -Berkeley – USA, DVD [Published].

Xu, H., Sonnenthal, E.L., Spycher, N., Pruess, K. (2004), "TOUGHREACT user's guide: a simulation program for nonisothermal multiphase reactive geochemical transport in variably saturated geologic media", Lawrence Berkeley National Laboratory Report LBNL-55460, 203 p.

APPENDIX

Kinetics of mineral precipitation and dissolution

The following kinetic rate law (Lasaga, 1984) is used for mineral dissolution and precipitation:

$$r_n = \pm m_n k_n A_n \left|1 - \Omega_n^{\theta}\right|^{\eta}$$

where m, k and A represent the instantaneous amount of mineral n (in mol), the rate constant (in mol/m²/S) and the reactive surface area (in m²/mol), respectively. Ω_n represents the saturation index of the mineral n ($\Omega_n = Q_n/K_n$). θ and η are two empirical positive parameters assumed equal to 1 (Palandri and Kharaka, 2004). Dependency of k_n with temperature and pH is given by:

$$k_n = k_{25}^{N} \exp\left[\frac{-Ea^{N}}{R}\left(\frac{1}{T} - \frac{1}{298.15}\right)\right]$$
$$+ k_{25}^{A} \exp\left[\frac{-Ea^{A}}{R}\left(\frac{1}{T} - \frac{1}{298.15}\right)\right] a_H^{n_A}$$
$$+ k_{25}^{B} \exp\left[\frac{-Ea^{B}}{R}\left(\frac{1}{T} - \frac{1}{298.15}\right)\right] a_H^{n_B}$$

where E_a is the activation energy (in J/mol), k_{25} is the rate constant at 25°C, R is the gas constant (8.314 J/mol/K), T is the temperature (in K) and a_H is the activity of H^+. The indices N, A and B refer to neutral, acid and alkali mechanisms, respectively.

Little information is currently available on the precipitation kinetics. Thus, precipitation rate laws only consider the neutral mechanism and, it is assumed that the parameters of the precipitation kinetics equal those of the dissolution ones. Moreover, some mineral precipitation reactions (as quartz one) are inhibited in favor of others more probable (as chalcedony one) at the PT conditions examined (Table 12). Mineral reactions proceed under kinetic conditions are listed in Table X, with the values of the kinetic parameters used for the modeling.

Table 12 :Kinetic parameters used for the modeling.

	Minerals	Acid Mechanism			Neutral Mechanism		Base Mechanism			Source
		log k25 [mol/m2.s]	**Ea** [kJ/mol]	**n** [-]	**log k25** [mol/m2.s]	**Ea** [kJ/mol]	**log k25** [mol/m2.s]	**Ea** [kJ/mol]	**n** [-]	
Mineral allowed to precipitate as **secondary phases** during the Triassic brines injection	**Calcite**	-0.30	14.40	1.000	-5.81	23.50	-3.48	35.40	1.000	Palandri and Kharaka (2004)
	Disordered dolomite	-3.19	36.10	0.500	-7.53	52.20	-5.11	34.80	0.500	
	Quartz*	–	–	–	-13.99	87.60	–	–	–	
	Albite_low*	-10.16	65.00	0.457	-12.56	69.80	-15.60	71.00	-0.572	
	K-feldspar**	-10.06	51.70	0.500	-12.41	38.00	-21.20	94.10	-0.823	
	Anhydrite	–	–	–	-3.19	14.30	–	–	–	
	Barite	-6.90	30.80	0.220	-7.90	30.80	–	–	–	
	Magnesite	-6.38	14.40	1.000	-9.34	23.50	-5.22	62.80	1.000	
	Chalcedony	–	–	–	-13.99	87.60	–	–	–	
	Gibbsite	-7.65	47.50	0.992	-11.50	61.20	-16.65	80.10	-0.784	
	Kaolinite	-11.31	65.90	0.777	-13.18	22.20	-17.05	17.90	-0.472	
	Montmorillonite-Na	-10.98	23.60	0.340	-12.78	35.00	-16.52	58.90	-0.400	
	Illite	-11.71	46.00	0.600	-15.05	14.00	-12.31	67.00	0.600	Kholer *et al.* (2003)

* Dissolution only: chalcedony and clays precipitation are assumed to be more likely than quartz and feldspars ones, respectively, at the TP conditions examined.

** Dissolution and precipitation in batch modeling and, dissolution only in the reactive transport modeling. Literature study made after batch modeling shows that K-feldspar precipitation is debatable at the TP conditions examined (Browne, 1978). Thus, we decided to inhibit it in the reactive transport modeling.

Values in grey: mechanisms not considered because negligible at the TP conditions studied.